ANL-99/21

Argonne National Laboratory

OXIDATION OF ZPPR FUEL CORROSION PRODUCTS: NATIONAL SPENT FUEL PROGRAM FY 1999 FINAL REPORT

by

T. C. TOTEMEIER

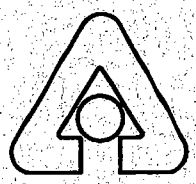

Argonne National Laboratory, Argonne, Illinois 60439
operated by the University of Chicago
for the United States Department of Energy under Contract W-31-109-Eng-38

Reproduced from the best available copy.

Available to DOE and DOE contractors from the
Office of Scientific and Technical Information
P.O. Box 62
Oak Ridge, TN 37831
Prices available from (423) 576-8401

Available to the public from the
National Technical Information Service
U. S. Department of Commerce
5285 Port Royal Road
Springfield, VA 22161

Distribution Category: UC-504
Materials

ANL-99/21

ARGONNE NATIONAL LABORATORY
P.O. Box 2528
Idaho Falls, Idaho 83403

Oxidation of ZPPR Fuel Corrosion Products: National Spent Nuclear Fuel Program FY 1999 Final Report

by

T.C. Totemeier

Engineering Division
Argonne National Laboratory - West

October 1999

TABLE OF CONTENTS

LIST OF FIGURES

LIST OF TABLES

Oxidation of ZPPR Fuel Corrosion Products:
National Spent Nuclear Fuel Program FY 1999 Final Report

by

T.C. Totemeier

ABSTRACT

The oxidation behavior of hydride-bearing corrosion products from uranium metal ZPPR fuel plates was studied in Ar-O_2, Ar-H_2O, Ar-O_2-H_2O, dry air, and moist air environments. Both isothermal and burning curve tests in the different environments were performed using a thermogravimetric analyzer. The effect of pre-oxidation in each environment on subsequent ignition temperature was investigated by performing burning curve tests on samples after isothermal oxidation. Low-temperature oxidation rates in Ar-O_2 and dry air environments were identical. Oxidation rates in moist environments were slightly higher, but the difference was not statistically significant at 95% confidence. Oxygen contamination was suspected to have lowered rates measured in the Ar-H_2O environment. Ignition temperatures measured in air were 10-15°C higher than those measured in Ar-20%O_2; the ignition temperatures of samples pre-oxidized in moist gas environments appeared to be slightly lower than those of unreacted samples at equivalent hydride fractions. Burning rates in all environments were linearly dependent on hydride surface area for surface areas less than 200 cm^2. Burning rates were constant at higher surface areas.

I. INTRODUCTION

This report presents the results of oxidation tests performed in FY 1999 on hydride-bearing U metal corrosion products formed on highly enriched uranium (HEU) fuel plates used in the Zero Power Physics Reactor (ZPPR). The primary goal of the tests was to measure the low-temperature (below ignition temperature) oxidation kinetics of the corrosion products in several different gaseous environments: Ar-O_2, Ar-H_2O, Ar-O_2-H_2O, dry air, and moist air. Uranium hydride will oxidize in environments containing oxygen and water vapor according to the following reactions:

$$UH_3 + O_2 \rightarrow UO_2 + \frac{3}{2} H_2 \quad (1)$$

$$UH_3 + 2H_2O \rightarrow UO_2 + \frac{7}{2} H_2 \quad (2)$$

The ignition and burning characteristics of the corrosion products before and after reaction in these environments were also measured. A second objective was to determine the effects of test sample mass on the ignition temperature and burning rates measured using a thermo-gravimetric analyzer (TGA).

The work described in this report represents the third year of research on the chemical reactivity of ZPPR fuel corrosion products funded by the National Spent Nuclear Fuel Program (NSNFP). Characterization of the corroded ZPPR plates and their associated corrosion products was performed in the first year [1, 2]; initial oxidation testing of the corrosion products in Ar-O_2 environments was performed in the second year [3, 4]. The corrosion products formed during extended vault storage of the U metal plates, which are clad in stainless steel jackets with porous metal endplugs. The presence of the cladding and access of the ambient gas environment (including water vapor) to the metal plates via the porous endplugs has led to severe localized corrosion and the presence of significant fractions of uranium hydride, UH_3, in the corrosion products. Because of the high UH_3 contents, these corrosion products represent a good test material for measuring the oxidation kinetics of UH_3 formed by corrosion of U metal. The oxidation kinetics and ignition characteristics of hydride-bearing U metal corrosion products are

currently of interest due to the extended underwater storage of certain metallic spent nuclear fuels (SNF) and the anticipated long-term storage of metallic SNF and U metal. Quantitative data describing the oxidation behavior of corrosion products is needed in the development of numerical codes which predict behavior of degraded metallic SNF under accident conditions.

The results of the first two years of research established the baseline oxidation behavior of the corrosion products [3]. A wide range of hydride fractions were observed, ranging from essentially none (for lightly corroded plates) to 61 wt% for a moderately corroded plate. Ignition of corrosion product samples from moderately corroded plates occurred at 140°C in Ar-20%O_2, while corrosion products samples from lightly corroded plates did not ignite. For the range of gas flows and oxygen concentrations initially investigated, the rate of burning following ignition was found only to be dependent on the net flow rate of O_2, implying that the rate was limited by convective O_2 transport to the sample. Oxidation rates below the ignition temperature were also measured; these rates were apparently independent of oxygen concentration between 4% and 20% O_2, and were slightly less than U metal oxidation rates on a surface area-normalized basis.

Considerably more information regarding the ZPPR fuel corrosion products and their oxidation behavior was obtained in an investigation of a pyrophoric event involving the products which occurred in 1998 [5]. In the course of the investigation, the ignition temperatures, hydride fractions, and burning rates of corrosion product samples from 21 separate containers were tested. The corrosion products in each container were collected from (typically) 40 plates. The average corrosion extent for the corrosion products in the various containers varied markedly. Briefly, the results of the investigation found that:

- The hydride fraction of the corrosion products increased with increasing corrosion extent of the source plates.
- The ignition temperature of the corrosion products decreased with increasing corrosion extent and hydride fraction.
- Ignition did not occur for hydride fractions less than 4 wt%.
- There was little change in corrosion product properties due to a room-temperature passivation step or vault storage.

The investigation presented in this report builds on the base established by the previous work by examining the oxidation behavior in different gas environments of interest, namely Ar-H_2O, Ar-O_2-H_2O, dry air, and moist air.

II. MATERIALS AND PROCEDURES

A. Materials Analyzed

The ZPPR corrosion products are a mixture of uranium oxide (nominally UO_{2+x}) and UH_3. A detailed description of the physical characteristics of the corrosion products is presented in ref. [2]. In this study, three different groups of corrosion products were used for testing. The amount of material in each group was sufficiently large that many samples of the group were available for TGA testing. The behavior of samples from a given group was very consistent. Detailed sampling procedures for three corrosion product groups are presented in refs. [3] and [5]. Table I summarizes information pertaining to the three groups.

TABLE I. Groups of Corrosion Products Tested

Material	Corrosion Extent (%)	Hydride Fraction (wt%)	Condition
Plate 3411	1.08	16-24	As-declad, stored in Ar.
Batch 2	1.41	15-18	Passivated at 25°C; stored in Ar.
Can RAM97-23/24	1.80	16-25	Passivated at 25°C; long-term vault storage in food-pack container.

The first group of corrosion products was obtained from ZPPR plate 3411. A total of 2.40 g of products were obtained from this plate, corresponding to a corrosion extent of 1.08%. For this study, corrosion extent is quantified as the mass of loose corrosion product divided by the total uranium mass of the plate or plates from which the corrosion products were collected. For batches of products from multiple plates, this figure represents an average extent. The

corrosion products from plate 3411 were tested in the as-declad condition. Plate 3411 was de-clad in an Ar atmosphere and the corrosion products were stored in an Ar glovebox until they were tested.

The second group of products was obtained from a set of five plates as part of the pyrophoric event investigation and is referred to as "batch 2." The products were collected in an Ar glovebox and were combined to form a single group. The total quantity of products was 15.62 g, corresponding to a corrosion extent of 1.41%. After collection, the batch 2 corrosion products underwent a room temperature passivation procedure, which entailed grinding using a mortar and pestle followed by a two-hour exposure to an Ar environment containing approximately 3% O_2. The results presented in ref. [5] demonstrate that this room temperature passivation procedure did not affect the oxidation behavior of the corrosion products (i.e. the products were not passivated).

The third group of corrosion products was obtained from can RAM97-23/24. These products were collected from 40 ZPPR plates during the ZPPR plate processing campaign described in ref. [5]. The 40 plates were de-clad in an Ar glovebox and "passivated" at room temperature according to the procedure described above. A total of 210.83 g of corrosion products were collected, corresponding to an average corrosion extent of 1.80%. After "passivation," the products were transferred to an air hood, where they were sealed into quart-size foodpack cans and placed into vault storage. Following the pyrophoric event of March 1998 involving similar corrosion products, all 21 cans remaining in vault storage, including RAM97-23/24, were removed and placed into an Ar glovebox. Samples of corrosion products from all cans were tested as part of the event investigation. Corrosion product samples from can RAM97-23/24 were used for tests investigating the effect of TGA sample mass on ignition and burning characteristics. As with the products from batch 2, the testing performed in ref. [5] showed that the behavior of the corrosion products vault-stored up to 2 years after undergoing the room temperature passivation procedure was essentially identical to that of the as-declad corrosion products.

B. Analysis Procedures

1. Gas Sorption Analysis

Gas sorption analysis using the Brunauer, Emmet, and Teller (BET) method was performed on corrosion products from plate 3411 and can RAM97-23/24 to measure their specific surface area, a parameter needed for analysis of the oxidation kinetics measured in a TGA test. Analysis was performed using a Quantachrome Quantasorb analyzer and standard BET techniques with Kr gas as the adsorbate, He gas as the carrier, and N_2 gas for calibration. Adsorption was carried out at liquid N_2 temperature; three consecutive measurements were made on each sample. BET tests were not performed on samples from Batch 2; for this material the specific surface area was assumed to be the most common value measured for other ZPPR corrosion product samples [3, 5], 0.75 m^2/g.

2. Oxidation Testing

Oxidation testing was performed using a modified Shimadzu TGA-51H analyzer located in a purified Ar glovebox. Details of the testing apparatus and analysis techniques are presented in refs. [1] and [3] A number of different gas environments were used in the present investigation. The gas environment in the TGA is controlled by varying the relative flow rates of reacting and purge gases. The purge gas flows through the balance area of the TGA and then into the sample area in order to cool the balance electronics. Ar is always used for the purge gas. The reacting gas enters into and mixes with the purge gas slightly before entering the sample area. The reacting gas supply line could be configured so that the reacting gas passed through a bubbler in order to introduce water vapor into the reacting gas. A total flow rate of 200 ml/min and a total pressure of 70 kPa (10 psia) was used for all tests. The configurations used for various gas environments are summarized in Table II and described below.

The baseline gas environment used was Ar-20%O_2. Most data previously reported in this program was obtained in this environment. An Ar-20%O_2 environment is

created by mixing an Ar-30%O_2 reacting gas at 133 ml/min with the pure Ar purge gas at 67 ml/min.

TABLE II. Reacting and Purge Gases for Different Gas Environments

Environment (vol%)	P_{H2O} (kPa)	Reacting Gas (vol%)	Reacting Gas Flow Rate (ml/min)	Bubbler? (Y/N)	Purge Gas	Purge Gas Flow Rate (ml/min)
Ar-20%O_2	0	Ar-30%O_2	133	N	Ar	67
Ar-4%H_2O	2.7	Ar-4.3% H_2O	180	Y	Ar	20
Ar-20%O_2-3%H_2O	2.0	Ar-28.7%O_2-4.3%H_2O	136	Y	Ar	64
Air-5%Ar	0	Air	190	N	Ar	10
Air-4%H_2O-5%Ar	2.9	Air-4.3%H_2O	190	Y	Ar	10

200 ml/min total flow rate for all tests.
70 kPa total pressure for all tests.

Moist inert gas testing was performed in a mixture of Ar and water vapor. This environment is created by passing a pure Ar reacting gas through the bubbler. The fraction of water vapor in the reacting gas is fixed by the saturated water vapor pressure at the temperature of the bubbler (25°C) and the total pressure in the reacting gas line. The saturated partial pressure of water vapor, p_{H2O}, at 25°C is 3.2 kPa [6] and the total reacting gas line pressure, p_{TOT}, is 70 kPa (10 psia; the TGA operates at a reduced pressure relative to ambient), therefore the water vapor fraction is: $x_{H2O} = p_{H2O}/p_{TOT} = 4.3\%$. This concentration is reduced by mixing with the purge gas. Mixing of the Ar-4.3%H_2O reacting gas at 180 ml/min with a pure Ar purge gas at 20 ml/min results in a final gas composition of Ar-3.9%H_2O (referred at as Ar-4%H_2O). At a total pressure of 70 kPa, the corresponding water vapor pressure is 2.7 kPa. Note that this water vapor pressure does not vary with test temperature; however, the relative humidity ($p_{H2O}/p_{H2O, SAT}$) will vary greatly with temperature due to the temperature dependence of the saturated water vapor pressure.

To obtain an Ar-O_2-H_2O gas environment, an Ar-30%O_2 reacting gas is passed through the bubbler to saturate it with water vapor and then is mixed with a pure Ar purge gas to lower the O_2 concentration to 20%. Again, the fraction of water vapor in the reacting gas after passing through the bubbler is 4.3%. In this case the water vapor is mixed with Ar-30%O_2 instead of Ar, resulting in an overall reacting gas composition of Ar-28.7%O_2-4.3%H_2O. To

obtain a final O_2 concentration of 20%, the water-saturated reacting gas at a flow rate of 136 ml/min is mixed with a pure Ar purge at 64 ml/min. The final gas composition is Ar-20%O_2-2.9%H_2O (referred to as Ar-20%O_2-3%H_2O). At a total pressure of 70 kPa, the corresponding water vapor pressure is 2.0 kPa.

A cylinder of compressed breathing air is used as the reacting gas for tests performed in dry and moist air. In order to obtain a nearly pure air test environment the Ar purge gas flow rate is reduced to 10 ml/min. When mixed with 190 ml/min of air, the final test environment is Air-5%Ar. To create the moist air reacting environment, the air is passed through the bubbler. The fraction of water vapor in the air after saturation at 25°C is 4.3%. The moist air reacting gas is mixed with a 10 ml/min Ar purge gas flow, resulting in a test environment of Air-4.1%H_2O-5%Ar (referred to as Air-4%H_2O-5%Ar), with a water vapor partial pressure of 2.9 kPa.

Oxidation tests were performed in isothermal and burning curve modes. In an isothermal test, the sample is heated to the test temperature in either the test environment or a pure Ar atmosphere. Heatup is performed in pure Ar when the test temperature is sufficiently high that significant oxidation will occur during heatup. When the test temperature is reached and stabilized, the reacting gas is admitted into the sample chamber by opening a solenoid valve in its supply line. The weight of the sample is recorded for the duration of the test. In this investigation, the duration of isothermal tests varied from 100 min to 3600 min. Longer test durations are required for low-temperature tests.

For isothermal tests in gas environments containing water vapor, the sample is pre-exposed to the test environment at 35°C for 500 or 900 min in order to insure that the oxide component of the sample is saturated with water prior to heating to the test temperature. Absorption of water vapor by the sample gives a spurious weight gain (i.e. not due to reaction of hydride). When the sample is subsequently heated to the test temperature the sample weight decreases due to thermal desorption of water. The weight loss only occurs during heating—once the temperature stabilizes, the sample weight begins to increase. Because the sample was pre-

saturated at a low temperature, all weight increase at the test temperature is assumed to result from hydride oxidation rather than water absorption.

The objective of the burning curve test is to measure the ignition temperature, burning rate, and hydride fraction of a sample. In a burning curve test the sample is heated at 15°C/min in a flowing atmosphere of either Ar-20%O_2 or Air-5%Ar while the sample weight and furnace control thermocouple temperature are monitored. Ignition of the sample is clearly indicated by a sharp, simultaneous increase in both values; the ignition temperature is defined as the furnace temperature at this point. The weight increase during burning is linear and referred to as the burning rate. The sample is allowed to oxidize to completion, which is indicated by the sample weight becoming stable. The total weight change during burning is used to calculate the fraction of hydride in the sample via the stoichiometry of the hydride-oxygen reaction. Burning curve tests were performed on every TGA sample. Some burning curve tests were performed on samples without pre-oxidation in order to establish the baseline characteristics of each group of corrosion products. Most burning curve tests were performed on samples after partial reaction in isothermal tests. The objective of these tests was to measure the hydride fraction of the sample (as described in ref. [3]) and also to determine the effects of partial reaction in the test environment on the subsequent ignition and burning characteristics of the sample.

III. RESULTS

A. Specific Surface Areas

The specific surface areas measured for plate 3411 and can RAM97-23/24 corrosion products were similar to those of a wide range of ZPPR corrosion products in several different conditions (e.g., as-declad, passivated, and vault-stored). The results of the three BET runs for plate 3411 corrosion products varied from 0.74 to 0.76 m^2/g, and the results for can RAM97-23/24 corrosion products varied from 0.83 to 0.84 m^2/g. The range of values previously observed was 0.5-1.0 m^2/g [3, 5].

B. Isothermal Oxidation Behavior

The shapes of weight gain versus time curves for most isothermal tests performed in this study were linear. A typical plot of weight gain versus time is shown in Figure 1. For some tests, however, the rate of weight gain tended to decrease slowly with time, similar to that reported previously [3]. The curvature was not consistent, so it was not possible to describe the oxidation kinetics for these tests using parabolic or paralinear rate laws. Instead, best linear fits were made to the weight gain versus time curves. Because the rate of weight gain did not change significantly over the course of a test, the error introduced by the somewhat arbitrary fit is small, especially relative to overall scatter in the rates as a function of temperature. To compute oxidation rates, the weight gain rates for all tests were normalized by each sample's hydride surface area, which was taken as the product of the specific surface area for the group of corrosion products from which the sample was taken, the sample mass, and the sample's hydride fraction. The hydride fraction was measured for each sample in a burning curve test performed after the isothermal test.

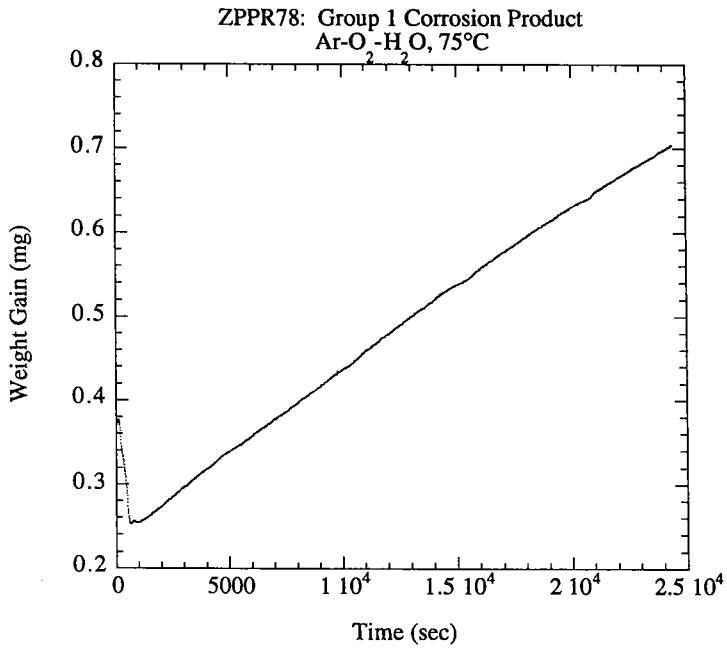

Figure 1. Plot of typical weight gain versus time for low-temperature oxidation of ZPPR corrosion products (ZPPR 78; Ar-20%O_2-3%H_2O, 75°C). Intial weight loss is due to water vapor desorption.

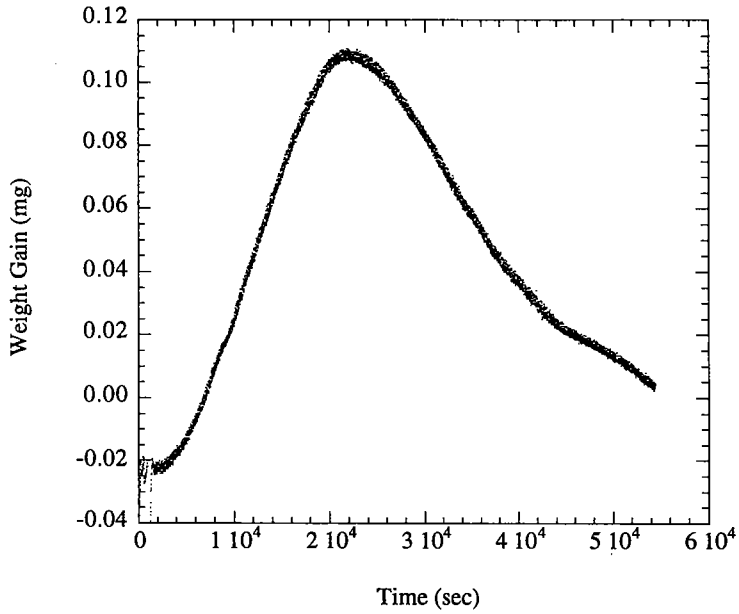

Figure 2. Example of erratic weight gain observed at very low temperatures (ZPPR 125; Air-5%Ar, 50°C).

For some tests at very low temperatures (35°C and 50°C), the rate of weight gain was so slow that the variation in the electronic zero of the TGA led to erratic weight gains. A typical example is shown in Figure 2. Oxidation rates are not reported for these tests, except for one test in which the duration of test was sufficiently long (3600 min) that a linear rate of weight gain could clearly be discerned through the background noise. Erratic weight behavior became more frequent in tests performed at the end of the investigation. Further investigation of this problem has shown that variations in the intensity of the photosensor light source in the TGA balance mechanism as it approached the end of its life led to fluctuations in the electronic zero of the TGA. The magnitude of the fluctuations was only significant for tests performed at 35°C and 50°C.

The dependence of oxidation rates on temperature is typically described using the Arrhenius expression:

$$k = A \exp(-Q/RT) \tag{1}$$

where k is the normalized linear oxidation rate, A is a pre-exponential factor, Q is the activation energy, R is the ideal gas constant, and T is absolute temperature. A linear regression fit to $\ln(k)$

versus $1/T$ yields $\ln(A)$ and $-Q/R$ as the intercept and slope, respectively, of the regression line. Table III shows values of $\ln(A)$ and Q determined for each unique set of isothermal oxidation data in this investigation and their associated standard errors and 95% confidence intervals.

1. Ar-20%O_2

Isothermal tests in an Ar-20%O_2 environment were performed on corrosion product samples from plate 3411 and batch 2. Table A-I in the Appendix shows individual test conditions and results for isothermal tests in Ar-20%O_2 and their associated burning curve tests (burning curve results are discussed below). Figure 3 shows an Arrhenius plot of normalized oxidation rate for all tests in Ar-O_2 environments versus inverse temperature. Data for the two separate groups of corrosion product fall within the same scatterband as previous data. The statistical equivalence of the oxidation rates was verified by comparing the Arrhenius parameters for the various groups of data against each other's 95% confidence intervals. All parameters fall within the confidence intervals. In order to provide the most accurate estimate of isothermal oxidation rates in Ar-20%O_2, the data from the separate corrosion product groups were combined. The resulting Arrhenius parameters are also shown in Table III.

2. Ar-4%H_2O

Isothermal tests in an Ar-4%H_2O environment were performed on corrosion products from plate 3411. Table A-II shows individual test conditions and results for isothermal tests in Ar-4%H_2O and their associated burning curve tests in Ar-20%O_2. The results of the pre-exposures at 35°C are shown as separate tests in Table A-II. The rates of weight gain shown for 35°C exposures correspond to later rates observed after the samples were believed to be saturated with water vapor. These rates were not plotted or included in the regression fits, however, due to the uncertainty regarding the true nature of the weight gain. Figure 4 is a comparison plot of the oxidation rates obtained in Ar-4%H_2O with those obtained in Ar-20%O_2. The data for Ar-H_2O appear to lie at the top of the scatterband for Ar-20%O_2, but the regression parameters for the two data sets fall within each other's 95% confidence intervals, so this apparent difference is not statistically significant at a 95% confidence level.

TABLE III. Rate Equation Parameters for Low-Temperature Oxidation

	$Ar-20\%O_2$ (3411)	$Ar-20\%O_2$ (Batch 2)	$Ar-20\%O_2$ (All)	$Ar-4\%H_2O$ (3411)	$Ar-20\%O_2-3\%H_2O$ (Batch 2)	$Air-5\%Ar$ (Batch 2)	$Air-4\%H_2O-5\%O_2$ (Batch 2)
No. of Data Points	4	6	15	6	6	9	8
ln(A)[a]	– 0.44	1.61	1.11	0.18	2.48	2.43	7.09
Std. Error for ln(A)	2.60	1.60	1.16	1.08	0.50	2.08	0.76
95% C.I. for ln(A)[b]	± 11.17	± 4.44	± 2.51	± 3.01	± 1.40	± 4.93	± 1.85
Q[c]	47.4	54.3	52.9	49.2	55.4	56.5	69.7
Std. Error for Q	7.96	4.80	3.55	3.32	1.50	6.48	2.32
95% C.I. for Q	± 34.3	± 13.3	± 7.67	± 9.22	± 4.16	± 12.8	± 5.67
R^2	0.947	0.970	0.945	0.982	0.997	0.915	0.993
Temperature Range	50-125°C	50-125°C	50-150°C	50-150°C	50-125°C	50-150°C	50-125°C

Linear Regression on $\ln(k) = \ln(A) + (-Q/R)(1/T)$; $k = A \exp(-Q/RT)$, where k is the linear oxidation rate.

a: Units of A are $mg/cm^2/sec$.

b: Confidence intervals are reported as a range about the mean value.

c: Units of Q are kJ/mol.

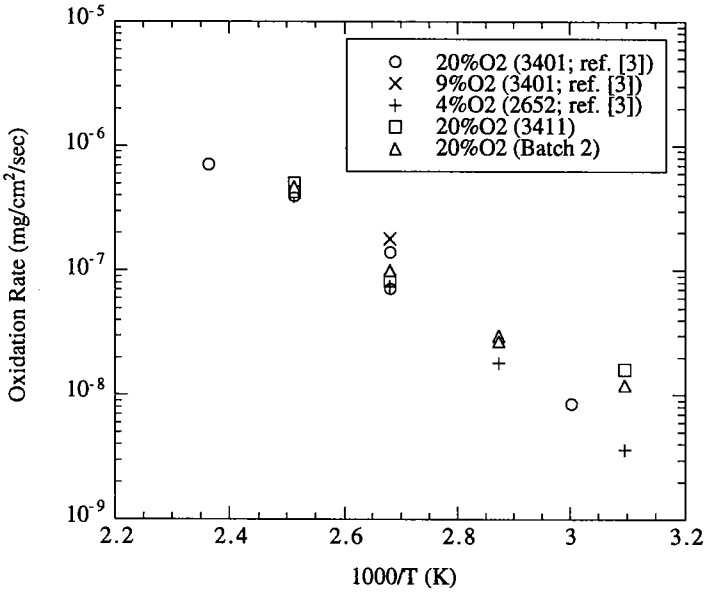

Figure 3. Low-temperature oxidation rates in Ar-O_2 environments versus reciprocal temperature.

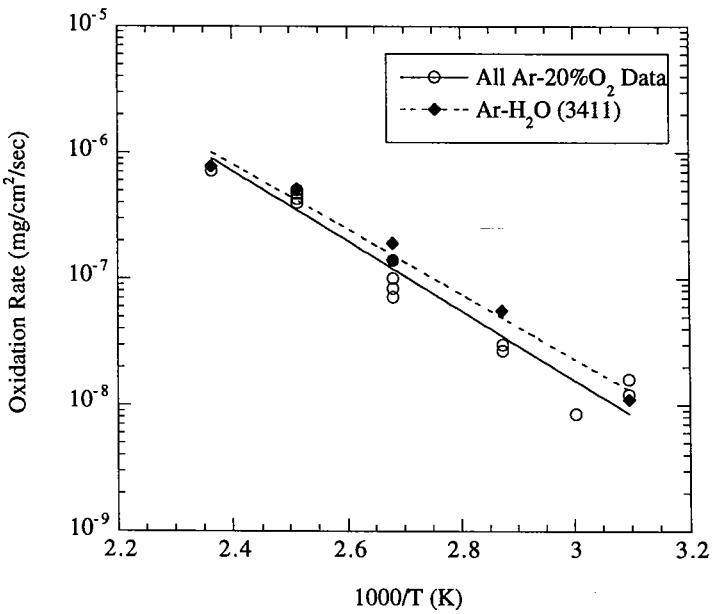

Figure 4. Comparison of low-temperature oxidation rates in Ar-4%H_2O and Ar-20%O_2.

3. Ar-20%O_2-3%H_2O

Isothermal tests in an Ar-20%O_2-3%H_2O environment were performed on corrosion products from batch 2. Table A-III shows individual test conditions and results for isothermal tests in Ar-20%O_2-3%H_2O and their associated burning curve tests in Ar-20%O_2. The results of the pre-exposures at 35°C are again shown as separate tests in Table A-III. Figure 5 is a comparison plot of the oxidation rates obtained in Ar-20%O_2-3%H_2O with those obtained in Ar-20%O_2. As with Ar-4%H_2O, the data for Ar-20%O_2-3%H_2O appear to lie at the top of the scatterband for Ar-20%O_2, but the regression parameters for the two data again sets fall within each other's 95% confidence intervals.

4. Air-5%Ar

Isothermal tests in an Air-5%Ar environment were performed on corrosion products from batch 2. Table A-IV shows individual test conditions and results for these tests and their associated burning curve tests, also performed in Air-5%Ar. Figure 6 is a comparison plot of the oxidation rates obtained in Air-5%Ar with those obtained in Ar-20%O_2. The data for the two environments fall within the same scatterband, and the Arrhenius parameters shown in Table III fall within each other's 95% confidence intervals. A regression fit to literature data for oxidation of U metal reported by Trimble [7] is also shown. Both the magnitude of the oxidation rates and the activation energy are slightly lower for the UH_3 data.

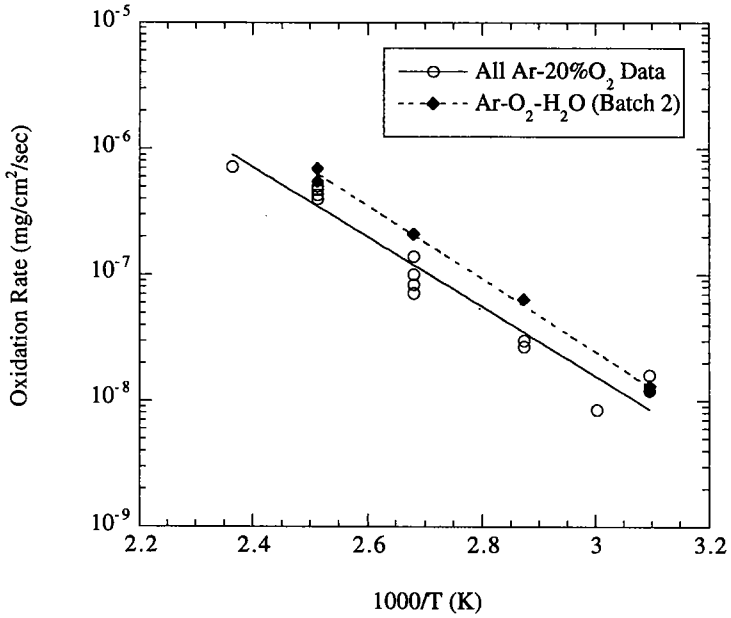

Figure 5. Comparison of low-temperature oxidation rates in Ar-20%O_2-3%H_2O and Ar-20%O_2.

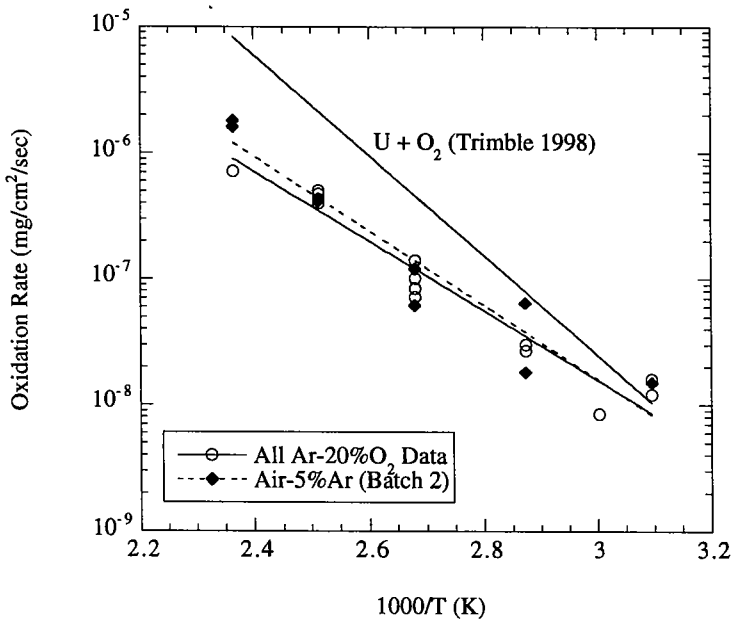

Figure 6. Comparison of low-temperature oxidation rates in Air-5%Ar and Ar-20%O_2. The regression fit to U metal literature data from Trimble [7] is also shown.

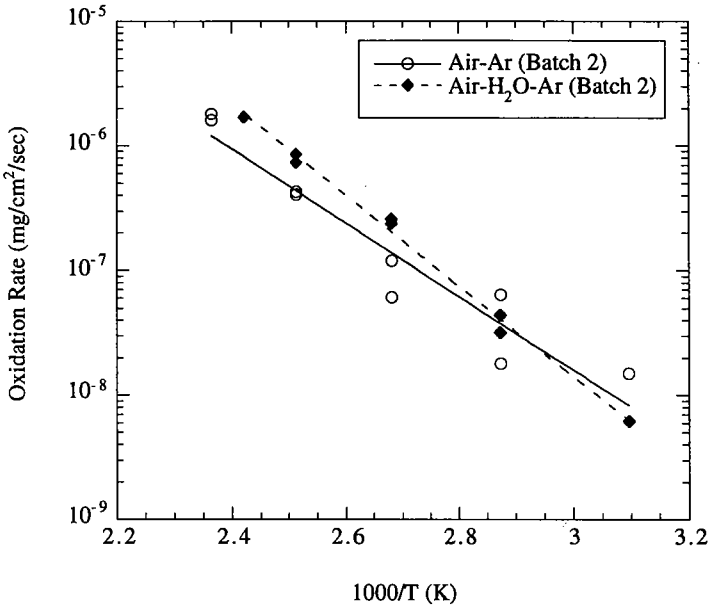

Figure 7. Comparison of low-temperature oxidation rates in Air-5%Ar and Air-4%H_2O-5%Ar.

5. Air-4%H_2O-5%Ar

Isothermal tests in an Air-4%H_2O-5%Ar environment were performed on corrosion products from batch 2. Table A-V shows individual test conditions and results for these tests and their associated burning curve tests in Air-5%Ar. The results of the pre-exposures at 35°C are shown as separate tests in Table A-V. Figure 7 is a comparison plot of the oxidation rates obtained in Air-4%H_2O-5%Ar with those obtained in Air-5%Ar. As with the data in Ar-H_2O and Ar-O_2-H_2O, the data for Air-4%H_2O-5%Ar lie at the top of and above the scatterband for Air-5%Ar. However, in this case the Arrhenius parameters for the two conditions (shown in Table III), do not lie within each other's 95% confidence intervals, but the boundaries of the confidence intervals overlap. To more accurately determine the statistical difference, if any, between the parameters, a t-test was performed using the procedure described in ref. [8] (page 76). The slope and intercept parameters were tested separately. In each case, the variances for the two data sets were pooled and the statistical significance of the difference in the parameters determined. Both the slope and intercept were not significantly different at a 95% confidence level, but were significantly different at a 90% confidence level, with both parameters in Air-4%H_2O-5%Ar higher than those in Air-5%Ar. Examination of the two sets of data shows that

the true difference, if any, between them is in the activation energy. The magnitude of the rates are similar, especially at low temperatures. A small difference in activation energy significantly affects the resulting intercept value.

C. Ignition Temperatures

1. Unreacted Products

As expected, the ignition temperatures of corrosion product samples from plate 3411 and batch 2 corrosion products in the unreacted condition (i.e., without pre-oxidation in an isothermal test) and an Ar-20%O_2 environment fell within the scatter of other ZPPR corrosion products tested in Ar-20%O_2 at equivalent hydride fractions [3, 5]. The ignition temperatures of unreacted batch 2 corrosion products tested in an Air-5%Ar environment were slightly greater than data obtained in Ar-20%O_2. The hydride fraction of batch 2 corrosion products was 17-18 wt%, and the ignition temperature in Air-5%Ar was between 167°C and 174°C. The ignition temperatures of unreacted products in Ar-20%O_2 with equivalent hydride fractions was between 159°C and 170°C. This difference is likely not statistically significant due to the scatter in the data.

2. Pre-oxidized Products

The objective of comparing ignition temperatures of pre-oxidized samples with those of unreacted samples is to determine the effects of exposure in the reacting environment of subsequent ignition temperature. Of particular interest is the difference between pre-oxidized and unreacted samples at equivalent hydride fractions. These differences were assessed using plots of ignition temperature versus hydride fraction, which provide a simple means of accounting for the dependence of ignition temperature on hydride fraction. The hydride fraction for pre-oxidized samples used to create these plots is that remaining after isothermal oxidation; the hydride fraction is computed only from the weight gain incurred in the burning curve test. The hydride fractions noted in the tables in the Appendix are the total initial fraction for the sample, computed from the sum of the weight gains in the isothermal and burning curve tests.

Figure 8 shows ignition temperature versus hydride fraction for plate 3411 and batch 2 corrosion products pre-oxidized in Ar-20%O_2 isothermal tests and subsequently burning curve tested. Data for unreacted (no pre-oxidation) corrosion products in Ar-20%O_2 are shown for comparison. The data for the two groups of pre-oxidized corrosion products generally lie within the scatter of the unreacted products at equivalent hydride fractions. The observed increases in ignition temperature after pre-oxidation were therefore solely due to the reduction in hydride fraction in the isothermal test from the initial, unreacted values of 17-18 wt% to values ranging from 4 to 18 wt%.

Ignition temperature data for plate 3411 products pre-oxidized in Ar-4%H_2O and batch 2 products pre-oxidized in Ar-20%O_2-3%H_2O are shown in Fig. 9, again compared against data for unreacted products in Ar-20%O_2. The data for samples pre-oxidized in Ar-4%H_2O have a large scatter, but some individual points lie beneath the curve for unreacted products, suggesting that for these samples there was a small increase in corrosion product reactivity due to reaction in Ar-4%H_2O. In contrast, the data for samples pre-oxidized in Ar-20%O_2-3%H_2O lie directly on the curve for unreacted products, confirming that the increases in ignition temperature were solely due to lowered hydride fraction.

Ignition temperature data for batch 2 corrosion products pre-oxidized in Air-5%Ar and Air-4%H_2O-5%Ar and burning curve tested in Air-5%Ar are shown Fig. 10, along with comparison data for unreacted products tested in Ar-20%O_2. The data for tests in Air-5%Ar lie above data in Ar-20%O_2, implying that ignition temperatures in air are somewhat higher than those in Ar-20%O_2. The difference is approximately 10-15°C for hydride fractions between 8% and 18%. Despite the large apparent gap, the difference is not statistically significant at 90% confidence due to the scatter in the data. The data for samples pre-oxidized in moist air have slightly lower ignition temperatures than samples pre-oxidized in dry air. The difference between the two data sets is also not significant at a 90% confidence level.

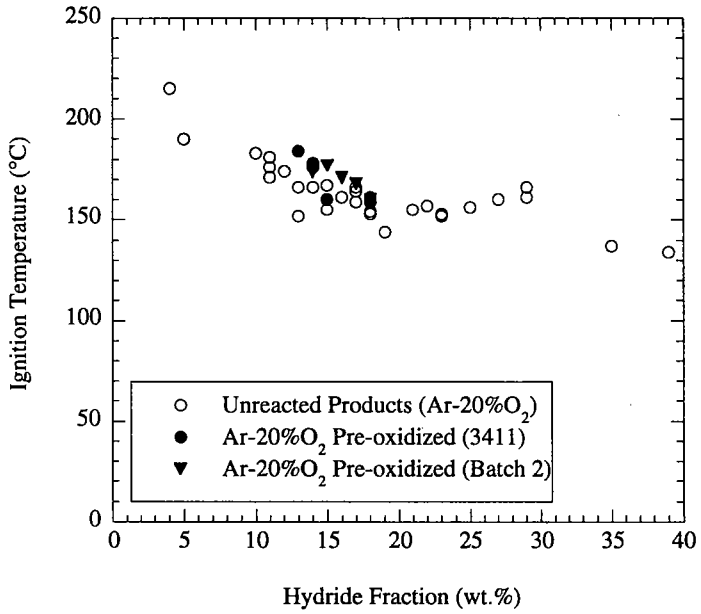

Figure 8. Comparison of ignition temperatures for samples pre-oxidized in Ar-20%O_2 with unreacted samples.

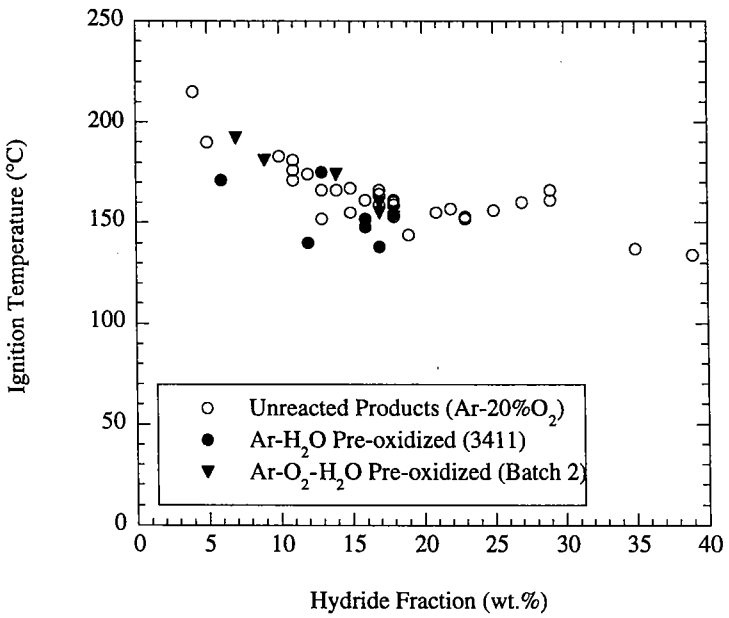

Figure 9. Comparison of ignition temperatures for samples pre-oxidized in Ar-4%H_2O and Ar-20%O_2-3%H_2O with unreacted samples.

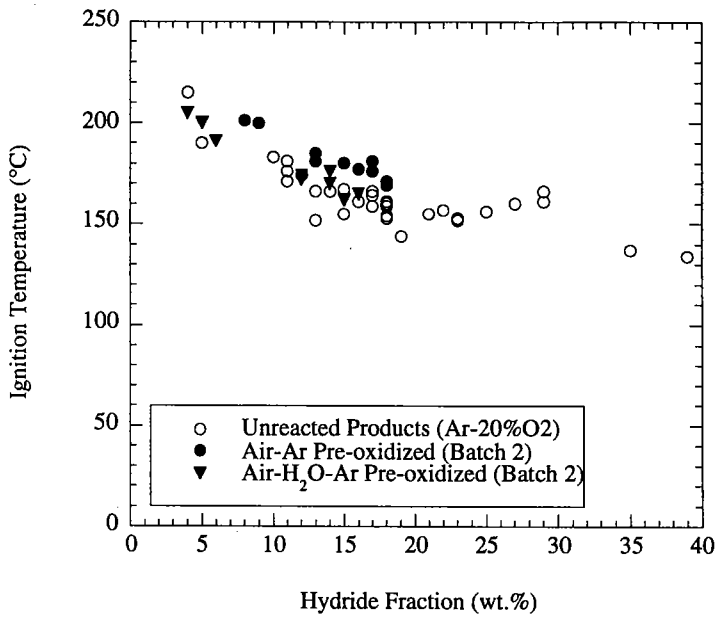

Figure 10. Comparison of ignition temperatures for samples pre-oxidized in Air-5%Ar and Air-4%H_2O-5%Ar with unreacted samples tested in Ar-20%O_2.

D. Burning Rates

The burning rates for the different corrosion product groups and test environments were compared using plots of burning rate versus sample hydride surface area. The burning rates measured in the initial TGA tests reported in ref. [3] were independent of hydride surface area, but additional tests performed in the pyrophoric event investigation and this study have shown that burning rates depend on hydride surface area for surface areas less than 200 cm^2. Above 200 cm^2 burning rates are relatively independent of surface area—all tests reported in ref. [3] had hydride surface areas greater than 200 cm^2. Figure 11 is a plot of burning rate versus hydride surface area showing data from all burning curve tests in this investigation. Data for all conditions fall into the same large scatterband, indicating that there is no effect of pre-oxidation or burning curve test environment (Ar-20%O_2 or Air-5%Ar) on burning rates.

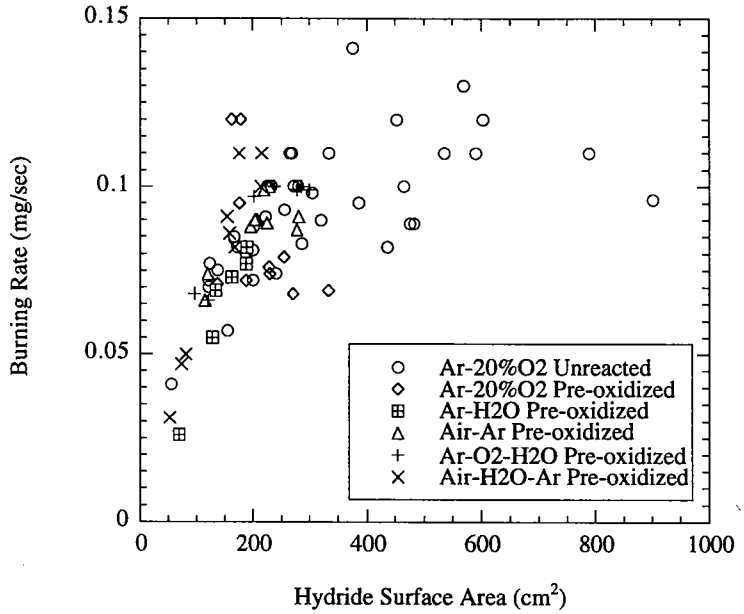

Figure 11. Burning rates versus hydride surface area for conditions investigated.

E. Effect of Sample Mass on Ignition and Burning

The results of the series of burning curve tests in Ar-20%O_2 on can RAM97-23/24 samples with varying sample mass are summarized in Figs. 12 and 13; individual test results are shown in Table A-VI. Figure 12 is a plot of ignition temperature as a function of sample mass. The ignition temperature decreases with increasing sample mass from zero to approximately 150 mg, and is independent of sample mass for samples greater than 150 mg. A similar effect is observed for burning rate (Fig. 13). For sample masses less than approximately 150 mg, burning rate increases with increasing sample mass. Burning rate appears to be independent of sample mass above approximately 150 mg. Note that all other isothermal and burning curve tests performed in this and previously studies used sample masses greater than 150 mg.

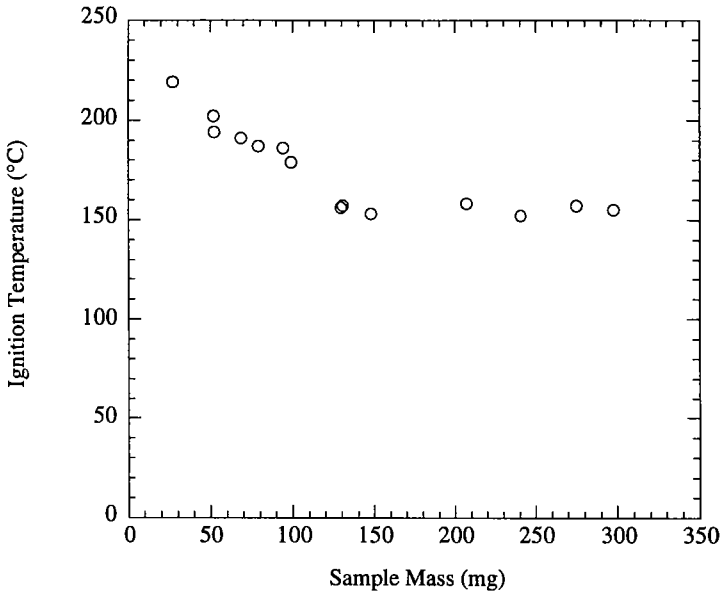

Figure 12. Effect of sample mass on ignition temperature for can RAM97-23/24 samples.

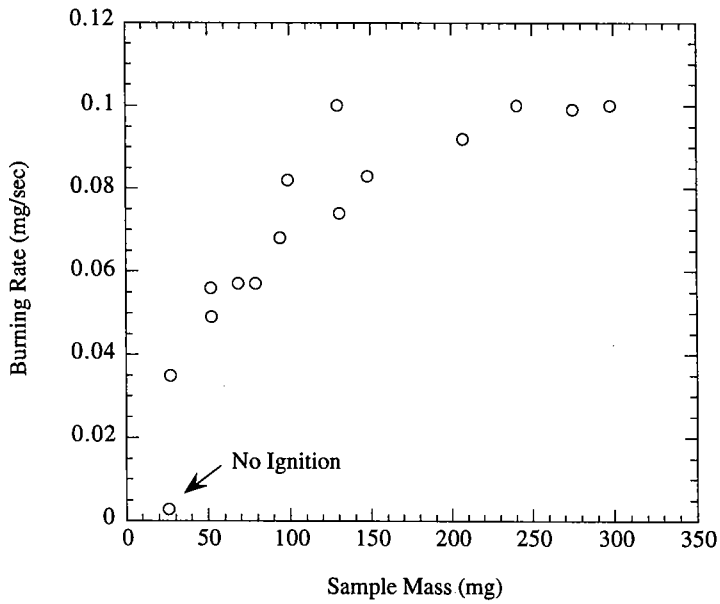

Figure 13. Effect of sample mass on burning rate for can RAM97-23/24 samples.

IV. DISCUSSION

A. Low-temperature Oxidation Rates

The results of the low-temperature oxidation tests imply that there is little difference between oxidation rates in Ar-20%O_2 and those in moist gas environments. The lack of a significantly higher oxidation rate in the Ar-H_2O environment is surprising since oxidation rates for U metal are more than an order of magnitude greater in water vapor than in oxygen. As shown in Fig. 6, oxidation rates for ZPPR corrosion products in Ar-20%O_2 are slightly less than those reported for U metal in air. A similar comparison may be made for rates in saturated water vapor. Figure 14 shows oxidation rates in the present study compared with literature rates for U metal in water vapor and mixtures of oxygen and saturated water vapor [7, 9]. The data for the ZPPR corrosion products lie considerably below the literature data for U metal in water vapor, although the activation energies are nearly identical. The rates for U metal in oxygen – water vapor mixtures show a markedly higher activation energy and are intermediate to between the UH_3 and U metal rates in water vapor. The reduction in the oxidation rate of U metal due to the presence of oxygen is marked, especially at lower temperatures.

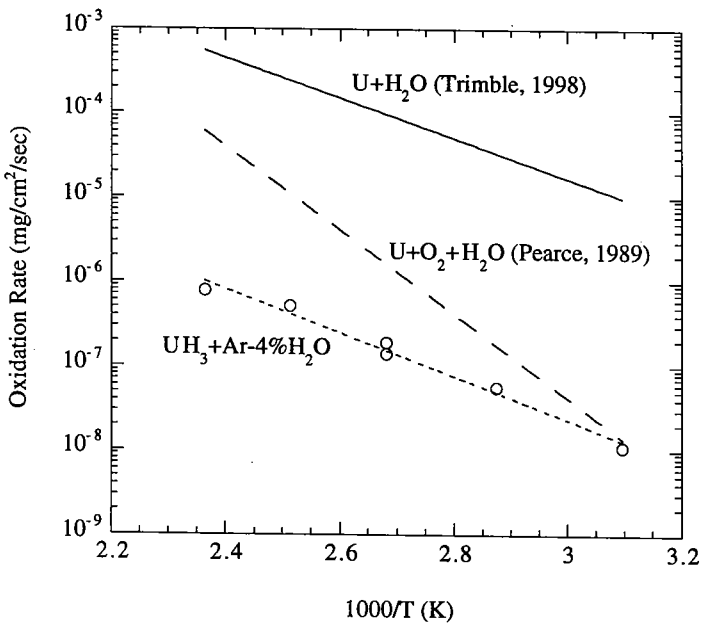

Figure 14. Comparison of oxidation rates of corrosion products in Ar-4%H_2O with literature data for U metal in H_2O.

While it is possible that there is an intrinsic difference in oxidation between UH_3 and U metal in water vapor, it appears much more likely that the data produced in this investigation do not accurately reflect true oxidation rates for ZPPR corrosion products in water vapor. It is well known that for U metal the presence of very small quantities of O_2 (100 ppm) in a water vapor test environment significantly retards the reaction rate [10, 11]. A similar effect may be present for UH_3 oxidation. The TGA test apparatus currently has no means to monitor or control the O_2 level in the sample chamber. Ultra-high purity Ar gas is fed through the bubbler to produce a moist inert reaction gas, but the potential for in-leakage of air into the reaction gas line is high because it operates at less than atmospheric pressure. The similarity of oxidation rates in the Ar-20%O_2-3%H_2O and Ar-4%H_2O environments supports the hypothesis that O_2 is present in the Ar-4%H_2O environment at levels sufficient to retard the oxidation rate. Modifications to the TGA are currently being made to ensure that the system is leak-tight and to provide for monitoring of O_2 levels in the reaction gas.

There was also no difference in low-temperature oxidation rates in an air environment relative to Ar-20%O_2, implying the carrier gas (Ar versus N_2) has little effect on low-temperature oxidation. This effect is also observed for U metal, for which low-temperature oxidation rates in air are essentially the same as those in pure O_2 [11]. The addition of water vapor to either the air or Ar-20%O_2 environment appeared to slightly accelerate oxidation rates. The difference in rates was only slight, and in fact was not statistically significant at 95% confidence.

B. Ignition Temperatures

The dependence of ignition temperature on hydride fraction was presented and discussed in the pyrophoric event investigation report [5]. The effects of pre-oxidation in Ar-20%O_2 on subsequent ignition temperature were also presented; the results of the tests on Plate 3411 corrosion products in this investigation confirm the earlier results. There is no intrinsic passivation effect for ZPPR corrosion products; increases in ignition temperature due to pre-oxidation can be accounted for by the lowered hydride fraction, and relatively large amounts of pre-oxidation result in only small increases in ignition temperature. For example, reaction of

half of the hydride for a sample with an initial hydride fraction of 20% results in an increase in ignition temperature of approximately 25°C. As demonstrated by data presented in ref. [5], reduction of hydride fractions to less than 4 wt% are required to prevent ignition. "Intrinsic passivation" refers to a large increase in ignition temperature of UH_3 due to formation of a very thin coherent oxide film which would not appreciably change the overall hydride fraction.

Ignition temperatures in air appear to be slightly greater at equivalent hydride fractions than those in Ar-20%O_2. This difference is not statistically significant due to the scatter in the data, but there does appear to be a definite separation in the data sets. The equivalence of low-temperature oxidation rates in air and Ar-20%O_2 suggests that any differences in ignition temperature are likely a result of the differences in the heat transfer properties of the carrier gases Ar and N_2, because all other heat generation and loss characteristics are the same. Numerical modeling is underway to assess these effects.

The results also indicate that there may be an intrinsic decrease in ignition temperature due to pre-oxidation in moist gas environments. The data for samples pre-oxidized in Ar-H_2O, Ar-20%O_2-3%H_2O, and Air-4%H_2O-5%Ar all lie below data Ar-20%O_2 and Air-5%Ar. The difference in reactivity is small and not statistically significant, but the consistent behavior in all three conditions suggests that a true effect may be present. The source of increased reactivity may be a less protective oxide formed during oxidation in environments containing water vapor than that formed in dry air or oxygen, hence leading to higher oxidation rates. Such an effect has been hypothesized to occur for U metal [12].

C. Burning Rates

As shown in Fig. 11, there was no effect of test environment (Ar-20%O_2 versus Air-5%Ar), corrosion product group, or pre-oxidation environment on burning rate. Burning rates were found to be dependent on hydride surface area for surface areas less than approximately 200 cm^2, and were independent at higher surface areas. The initial TGA testing [3] found that burning rates were dependent only on the net rate of oxygen flow, and not on surface area. In these prior tests, however, the hydride surface areas of all samples were greater than 200 cm^2.

The dependence implies that the burning rates for ZPPR corrosion products with total surface areas less than 200 cm^2 is limited by a process which is proportional only to the surface area of hydride present in the sample (as shown in ref. [3], above 200 cm^2 the burning rate is limited by convective O_2 transport). This is supported by the fact that samples with constant total surface area but varying hydride fractions fall onto the same curve as samples with constant hydride fraction but varying total surface area. The one common factor is hydride surface area. One possible rate-limiting step that would be dependent on hydride surface area is diffusion of O_2 through a boundary layer at the hydride particle surface.

Figure 15 is a plot of burning rates for all samples tested in Ar-20%O_2 or Air-5%Ar. Only the region for zero to 200 cm^2 is shown. The dependence of burning rate on hydride surface area is roughly linear. The slope of the line fit to this set of data is 5×10^{-4} $mg/cm^2/sec$. This rate is approximately 300 times higher than the low-temperature oxidation rate at 150°C. If it is assumed that oxidation during burning follows the same rate law as low-temperature oxidation, the burning temperature equivalent to an oxidation rate of $5x10^{-4}$ $mg/cm^2/sec$ is approximately 460°C. This figure agrees well with the actual sample temperature measured during burning in Ar-20%O_2 in the initial TGA study, which was 487°C [3].

The implications of these observations are uncertain. While it is possible that burning rates at low total surface areas are limited by a process such as oxygen diffusion, it is also possible that the heat balance characteristics of the samples tested are serendipitously similar, so that a small sample with higher hydride fraction burns at nearly the same rate as a larger sample with a lower hydride fraction. The relatively narrow range of hydride contents and sample sizes investigated prevents definitive conclusions from being reached. Hopefully numerical modeling underway will provide for better interpretation of the data.

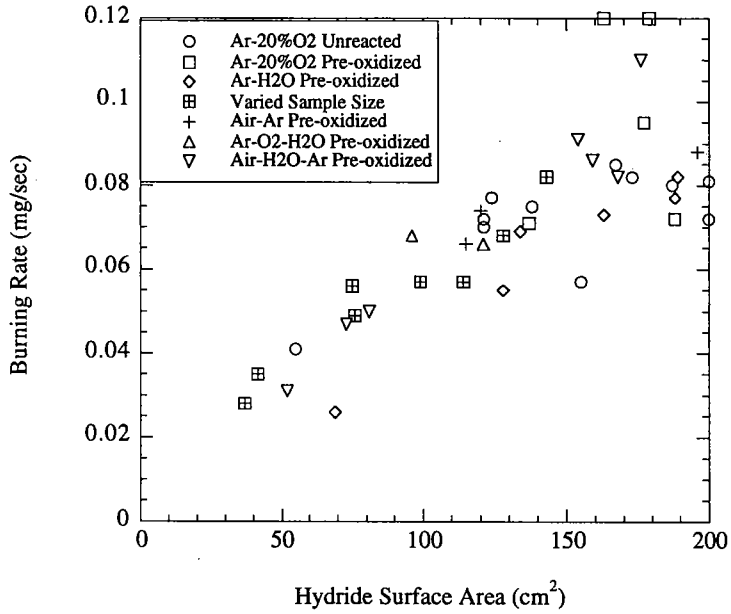

Figure 15. Burning rates versus hydride surface area for all tests with hydride surface areas less than 200 cm^2.

V. CONCLUSIONS

This report presented data obtained on the oxidation behavior of ZPPR corrosion products in fiscal year 1999. Isothermal and burning curve oxidation tests were performed in Ar-O_2, Ar-H_2O, Ar-O_2-H_2O, Air, and Air-H_2O environments. The following conclusions were reached:

1. Slightly higher oxidation rates were observed in Ar-4%H_2O and Ar-20%O_2-3%H_2O environments compared to Ar-20%O_2. The difference was not statistically significant at a 95% confidence level due to the relatively large scatter in the data. Oxygen contamination was suspected to have lowered rates measured in the Ar-H_2O environment.

2. Oxidation rates measured in an Air-5%Ar environment were equivalent to rates measured in Ar-20%O_2. Rates measured in Air-4%H_2O-5%Ar were slightly higher than rates in Air-5%Ar. Again, the difference was not significant at a 95% confidence level.

3. Burning curve ignition temperatures in Air-5%Ar were 10°C to 15°C higher than in Ar-20%O_2 at equivalent hydride fractions.

4. The ignition temperatures of samples pre-oxidized in moist gas environments appeared to be slightly lower than unreacted samples at equivalent hydride fractions. After accounting for changes in hydride fraction, there was no effect of pre-oxidation in Ar-20%O_2 or Air-5%Ar.

5. Burning rates in all environments were linearly dependent on hydride surface area for surface areas less than 200 cm^2. The normalized rate of burning in this range is 5×10^{-4} $mg/cm^2/sec$. Burning rates were constant at higher surface areas—the rate is limited by the net flow rate of O_2 in the TGA system.

ACKNOWLEDGEMENTS

The author wishes to acknowledge R.J. Briggs, E.A. Belnap, and R. Gonzales for their work in preparing safety documentation and sampling the ZPPR corrosion products, R.G. Pahl for helpful advice and review of this report, and the National Spent Nuclear Fuel Program for providing financial support for the project.

REFERENCES

[1] T.C. Totemeier, R.G. Pahl, S.L. Hayes, and S.M. Frank, *Metallic Uranium ZPPR Fuel: Corrosion Characteristics and Corrosion Product Oxidation Kinetics*, Argonne National Laboratory Report ANL-98/11 (1998).

[2] T.C. Totemeier, R.G. Pahl, S.L. Hayes, and S.M. Frank, J. Nucl. Mater. 256 (1998) 87.

[3] T.C. Totemeier and R.G. Pahl, J. Nucl. Mater. 265 (1999) 308.

[4] T.C. Totemeier and R.G. Pahl, "Oxidation Kinetics of Reaction Products Formed in Uranium Metal Corrosion," Proc. ANS Topical Meeting on *DOE Spent Nuclear Fuel and Fissile Materials Management*, Charleston, SC, Sept. 8-11, 1998, p. 271.

[5] T.C. Totemeier, *Characterization of Uranium Corrosion Products Involved in the March 13, 1998 Fuel Manufacturing Facility Pyrophoric Event*, Argonne National Laboratory Report ANL-99/7 (1999).

[6] D.R. Lide, ed., *CRC Handbook of Chemistry and Physics*, 71st Edition (CRC Press, Boca Raton, 1990), p.6-12.

[7] D.J. Trimble, *Reaction Rate Constant for Uranium in Water and Water Vapor*, Duke Engineering and Services Hanford, Inc. Report HNF-2853 (1998).

[8] J.K. Taylor, *Statistical Techniques for Data Analysis* (Lewis Publishers, Inc, Boca Raton, 1990).

[9] R.J. Pearce, *A Review of the Rates of Reaction of Unirradiated Uranium in Gaseous Atmospheres*, Central Electricity Generating Board Report RD/B/6231/R89 (1989).

[10] M. Baker, L.N. Less, and S. Orman, Trans. Faraday Soc. 62 (1966) 2525.

[11] C.A. Colmenares, Prog. Solid State Chem. 15 (1984) 257.

[12] T. Kondo, F.H. Beck, and M.G. Fontana, Corrosion 30 (1974) 330.

TABLE A-I. Test matrix and results for oxidation in Ar-20%O_2

Test ID	Material	Sample Weight (mg)	Hydride Surface (cm^2)	Test Type	Test Temp. (°C)	Test Time (min)	Ignition Temp. (°C)	Kinetics	Burning Rate (mg/sec)	Oxidation Rate ($mg/cm^2/sec$)	Wt. Gain (mg)	Hydride Fraction (%)
ZPPR 40	Plate 3411	176.2	260	Burning Curve	15°C/min	N/A	144	Linear	9.30E-02	N/A	5.7	19
ZPPR 41	Plate 3411	139.2	170	Burning Curve	15°C/min	N/A	166	Linear	8.20E-02	N/A	3.9	17
ZPPR 42	Plate 3411	172.3	230	Isothermal	125	120	N/A	Linear	N/A	5.00E-07	0.95	18
ZPPR 43	Plate 3411	172.3	230	Burning Curve	15°C/min	N/A	178	Linear	9.50E-02	N/A	5.1	18
ZPPR 44	Plate 3411	160.4	190	Isothermal	50	600	N/A	Decreasing Rate	N/A	1.60E-08	0.14	16
ZPPR 45	Plate 3411	160.4	190	Burning Curve	15°C/min	N/A	160	Linear	1.20E-01	N/A	4.3	16
ZPPR 46	Plate 3411	143.6	180	Isothermal	125	200	N/A	Decreasing Rate	N/A	4.30E-07	0.95	17
ZPPR 47	Plate 3411	143.6	180	Burning Curve	15°C/min	N/A	184	Linear	7.10E-02	N/A	4.0	17
ZPPR 48	Plate 3411	158.4	210	Isothermal	100	600	N/A	Decreasing Rate	N/A	8.40E-08	0.88	18
ZPPR 49	Plate 3411	158.4	210	Burning Curve	15°C/min	N/A	176	Linear	1.20E-01	N/A	4.7	18
ZPPR 91	Batch 2	200.3	270	Isothermal	75	400	N/A	Decreasing Rate	N/A	3.00E-08	0.25	18
ZPPR 92	Batch 2	200.3	270	Burning Curve	15°C/min	N/A	168	Linear	7.90E-02	N/A	6.0	18
ZPPR 93	Batch 2	195.9	270	Isothermal	75	400	N/A	Linear	N/A	2.70E-08	0.23	18
ZPPR 94	Batch 2	195.9	270	Burning Curve	15°C/min	N/A	168	Linear	6.90E-02	N/A	6.0	18
ZPPR 95	Batch 2	191.7	260	Isothermal	100	300	N/A	Linear	N/A	1.00E-07	0.61	18
ZPPR 96	Batch 2	191.7	260	Burning Curve	15°C/min	N/A	171	Linear	7.40E-02	N/A	5.8	18
ZPPR 97	Batch 2	200.9	270	Isothermal	50	600	N/A	Decreasing Rate	N/A	1.20E-08	0.12	18
ZPPR 98	Batch 2	200.9	270	Burning Curve	15°C/min	N/A	160	Linear	6.80E-02	N/A	6.1	18
ZPPR 99	Batch 2	203.7	260	Isothermal	125	100	N/A	Linear	N/A	4.30E-07	0.78	17
ZPPR 100	Batch 2	203.7	260	Burning Curve	15°C/min	N/A	177	Linear	7.60E-02	N/A	5.8	17
ZPPR 101	Batch 2	178.6	230	Isothermal	125	100	N/A	Linear	N/A	4.70E-07	0.82	17
ZPPR 102	Batch 2	178.6	230	Burning Curve	15°C/min	N/A	174	Linear	7.20E-02	N/A	5.2	17

Note: Hydride fraction shown is the total initial hydride fraction in the sample, computed from the sum of weight gains in the isothermal and burning curve tests.

TABLE A-II. Test matrix and results for oxidation in Ar-4%H_2O

Test ID	Material	Sample Weight (mg)	Hydride Surface (cm^2)	Test Type	Test Temp. (°C)	Test Time (min)	Ignition Temp. (°C)	Kinetics	Burning Rate (mg/sec)	Oxidation Rate ($mg/cm^2/sec$)	Wt. Gain (mg)	Hydride Fraction (%)
ZPPR50	Plate 3411	130.3	230	H_2O Saturation	35	900	N/A	Decreasing Rate	N/A	3.61E-09	0.17	24
ZPPR51	Plate 3411	130.3	230	Isothermal	100	600	N/A	Linear	N/A	1.43E-07	1.38	24
ZPPR52	Plate 3411	130.3	230	Burning Curve	15°C/min	N/A	138	Linear	7.30E-02	N/A	5.2	24
ZPPR53	Plate 3411	158.1	201	H_2O Saturation	35	900	N/A	Decreasing Rate	N/A	1.88E-09	0.19	17
ZPPR54	Plate 3411	158.1	201	Isothermal	50	600	N/A	Linear	N/A	1.12E-08	0.07	17
ZPPR55	Plate 3411	158.1	201	Burning Curve	15°C/min	N/A	152	Linear	8.20E-02	N/A	4.5	17
ZPPR56	Plate 3411	151.8	196	H_2O Saturation	35	900	N/A	Decreasing Rate	N/A	7.40E-09	0.39	17
ZPPR57	Plate 3411	151.8	196	Isothermal	150	300	N/A	Decreasing Rate	N/A	7.70E-07	2.59	17
ZPPR58	Plate 3411	151.8	196	Burning Curve	15°C/min	N/A	171	Linear	2.60E-02	N/A	4.4	17
ZPPR59	Plate 3411	140.0	165	H_2O Saturation	35	900	N/A	Decreasing Rate	N/A	6.90E-09	0.15	16
ZPPR60	Plate 3411	140.0	165	Isothermal	100	300	N/A	Linear	N/A	1.90E-07	0.54	16
ZPPR61	Plate 3411	140.0	165	Burning Curve	15°C/min	N/A	175	Linear	6.90E-02	N/A	3.7	16
ZPPR62	Plate 3411	141.1	171	H_2O Saturation	35	900	N/A	Decreasing Rate	N/A	3.80E-09	0.14	16
ZPPR63	Plate 3411	141.1	171	Isothermal	125	200	N/A	Linear	N/A	5.10E-07	1.03	16
ZPPR64	Plate 3411	141.1	171	Burning Curve	15°C/min	N/A	140	Linear	5.50E-02	N/A	3.8	16
ZPPR65	Plate 3411	155.0	211	H_2O Saturation	35	900	N/A	Decreasing Rate	N/A	6.11E-09	0.38	18
ZPPR66	Plate 3411	155.0	211	Isothermal	75	600	N/A	Decreasing Rate	N/A	5.60E-08	0.32	18
ZPPR67	Plate 3411	155.0	211	Burning Curve	15°C/min	N/A	148	Linear	7.70E-02	N/A	4.7	18

Note: Hydride fraction shown is the total initial hydride fraction in the sample, computed from the sum of weight gains in the isothermal and burning curve tests. All burning curve tests performed in Ar-20%O_2 at 200 ml/min.

TABLE A-III. Test matrix and results for oxidation in Ar-20%O_2-4%H_2O

Test ID	Material	Sample Weight (mg)	Hydride Surface (cm^2)	Test Type	Test Temp. (°C)	Test Time (min)	Ignition Temp. (°C)	Kinetics	Burning Rate (mg/sec)	Oxidation Rate ($mg/cm^2/sec$)	Wt. Gain (mg)	Hydride Fraction (%)
ZPPR71	Batch 2	182.7	228	H_2O Saturation	35	900	N/A	Decreasing Rate	N/A	9.40E-09	0.26	17
ZPPR72	Batch 2	182.7	228	Isothermal	125	300	N/A	Decreasing Rate	N/A	5.50E-07	3.1	17
ZPPR73	Batch 2	182.7	228	Burning Curve	15°C/min	N/A	192	Linear	6.80E-02	N/A	5.1	17
ZPPR74	Batch 2	192.8	241	H_2O Saturation	35	900	N/A	Decreasing Rate	N/A	7.50E-09	0.22	17
ZPPR75	Batch 2	192.8	241	Isothermal	100	300	N/A	Decreasing Rate	N/A	2.10E-07	1.02	17
ZPPR76	Batch 2	192.8	241	Burning Curve	15°C/min	N/A	174	Linear	9.70E-02	N/A	5.4	17
ZPPR77	Batch 2	217.5	299	H_2O Saturation	35	500	N/A	Decreasing Rate	N/A	7.10E-09	0.37	18
ZPPR78	Batch 2	217.5	299	Isothermal	75	400	N/A	Linear	N/A	6.40E-08	0.45	18
ZPPR79	Batch 2	217.5	299	Burning Curve	15°C/min	N/A	160	Linear	9.90E-02	N/A	6.7	18
ZPPR80	Batch 2	212.0	281	H_2O Saturation	35	500	N/A	Decreasing Rate	N/A	1.20E-08	0.29	18
ZPPR81	Batch 2	212.0	281	Isothermal	50	600	N/A	Linear	N/A	1.30E-08	0.14	18
ZPPR82	Batch 2	212.0	281	Burning Curve	15°C/min	N/A	153	Linear	1.00E-01	N/A	6.3	18
ZPPR83	Batch 2	179.0	219	H_2O Saturation	35	500	N/A	Decreasing Rate	N/A	9.40E-09	0.19	16
ZPPR84	Batch 2	179.0	219	Isothermal	125	200	N/A	Decreasing Rate	N/A	6.90E-07	2.27	16
ZPPR85	Batch 2	179.0	219	Burning Curve	15°C/min	N/A	181	Linear	6.60E-02	N/A	4.9	16
ZPPR86	Batch 2	186.5	241	H_2O Saturation	35	500	N/A	Decreasing Rate	N/A	9.10E-09	0.25	17
ZPPR87	Batch 2	186.5	241	Isothermal	50	600	N/A	Decreasing Rate	N/A	1.20E-08	0.1	17
ZPPR88	Batch 2	186.5	241	Burning Curve	15°C/min	N/A	155	Linear	1.00E-01	N/A	5.4	17

Note: Hydride fraction shown is the total initial hydride fraction in the sample, computed from the sum of weight gains in the isothermal and burning curve tests.
All burning curve tests performed in Ar-20%O_2 at 200 ml/min.

TABLE A-IV. Test matrix and results for oxidation in Air-5%Ar

Test ID	Material	Sample Weight (mg)	Hydride Surface (cm^2)	Test Type	Test Temp. (°C)	Test Time (min)	Ignition Temp. (°C)	Kinetics	Burning Rate (mg/sec)	Oxidation Rate ($mg/cm^2/sec$)	Wt. Gain (mg)	Hydride Fraction (%)
ZPPR 103	Batch 2	199.6	272	Burning Curve	15°C/min	N/A	169	Linear	1.10E-01	N/A	6.1	18
ZPPR 104	Batch 2	212.3	277	Burning Curve	15°C/min	N/A	167	Linear	1.00E-01	N/A	6.2	17
ZPPR 105	Batch 2	170.2	223	Burning Curve	15°C/min	N/A	174	Linear	9.60E-02	N/A	5	17
ZPPR 106	Batch 2	211.2	277	Burning Curve	15°C/min	N/A	167	Linear	1.00E-01	N/A	6.2	17
ZPPR 107	Batch 2	205.9	272	Isothermal	50	600	N/A	Erratic*	N/A	1.50E-08	0.09	18
ZPPR 108	Batch 2	205.9	272	Burning Curve	15°C/min	N/A	171	Linear	8.70E-02	N/A	6.1	18
ZPPR 109	Batch 2	207.8	281	Isothermal	75	600	N/A	Linear	N/A	1.80E-08	0.13	18
ZPPR 110	Batch 2	207.8	281	Burning Curve	15°C/min	N/A	169	Linear	9.10E-02	N/A	6.3	18
ZPPR 111	Batch 2	176.6	232	Isothermal	100	300	N/A	Linear	N/A	6.10E-08	0.43	18
ZPPR 112	Batch 2	176.6	232	Burning Curve	15°C/min	N/A	181	Linear	8.90E-02	N/A	5.2	18
ZPPR 113	Batch 2	191.9	241	Isothermal	150	100	N/A	Linear	N/A	1.60E-06	3	17
ZPPR 114	Batch 2	191.9	241	Burning Curve	15°C/min	N/A	201	Linear	6.60E-02	N/A	5.4	17
ZPPR 115	Batch 2	213.7	277	Isothermal	125	200	N/A	Linear	N/A	4.30E-07	1.6	17
ZPPR 116	Batch 2	213.7	277	Burning Curve	15°C/min	N/A	185	Linear	9.00E-02	N/A	6.2	17
ZPPR 117	Batch 2	201.0	259	Isothermal	125	200	N/A	Linear	N/A	4.10E-07	1.4	17
ZPPR 118	Batch 2	201.0	259	Burning Curve	15°C/min	N/A	181	Linear	8.80E-02	N/A	5.8	17
ZPPR 119	Batch 2	203.1	263	Isothermal	100	300	N/A	Linear	N/A	1.20E-07	0.65	17
ZPPR 120	Batch 2	203.1	263	Burning Curve	15°C/min	N/A	180	Linear	1.00E-01	N/A	5.9	17
ZPPR 121	Batch 2	169.6	219	Isothermal	75	600	N/A	Erratic*	N/A	6.40E-08	0.29	17
ZPPR 122	Batch 2	169.6	219	Burning Curve	15°C/min	N/A	177	Linear	9.00E-02	N/A	4.9	17
ZPPR 123	Batch 2	178.3	223	Isothermal	150	100	N/A	Linear	N/A	1.80E-06	2.4	17
ZPPR 124	Batch 2	178.3	223	Burning Curve	15°C/min	N/A	200	Linear	7.40E-02	N/A	5	17

*: Erratic rate too low for meaningful measurement.

Note: Hydride fraction shown is the total initial hydride fraction in the sample, computed from the sum of weight gains in the isothermal and burning curve tests. All burning curve tests performed in Air-5%Ar at 200 ml/min.

TABLE A-V. Test matrix and results for oxidation in Air-4%H_2O-5%Ar

Test ID	Material	Sample Weight (mg)	Hydride Surface (cm^2)	Test Type	Test Temp. (°C)	Test Time (min)	Ignition Temp. (°C)	Kinetics	Burning Rate (mg/sec)	Oxidation Rate ($mg/cm^2/sec$)	Wt. Gain (mg)	Hydride Fraction (%)
ZPPR 134	Batch 2	193.5	223	Isothermal	35	500	N/A	Erratic[a]	N/A	N/A	N/A	15
ZPPR 135	Batch 2	193.5	223	Isothermal	125	300	N/A	Linear	N/A	8.50E-07	3.39	15
ZPPR 136	Batch 2	193.5	223	Burning Curve	15°C/min	N/A	200	Linear	4.70E-02	N/A	5	15
ZPPR 137	Batch 2	170.5	192	Isothermal	35	500	N/A	Linear	N/A	2.70E-08	0.46	15
ZPPR 138	Batch 2	170.5	192	Isothermal	100	300	N/A	Linear	N/A	2.60E-07	0.86	15
ZPPR 139	Batch 2	170.5	192	Burning Curve	15°C/min	N/A	174	Linear	9.10E-02	N/A	4.3	15
ZPPR 140	Batch 2	167.6	188	Isothermal	35	500	N/A	Erratic[a]	N/A	N/A	N/A	15
ZPPR 141	Batch 2	167.6	188	Isothermal	75	600	N/A	Linear	N/A	4.40E-08	0.21	15
ZPPR 142	Batch 2	167.6	188	Burning Curve	15°C/min	N/A	170	Linear	1.10E-01	N/A	4.2	15
ZPPR 143	Batch 2	190.1	219	Isothermal	35	500	N/A	Linear	N/A	4.00E-08	0.43	15
ZPPR 144	Batch 2	190.1	219	Isothermal	50	900	N/A	Erratic[a]	N/A	N/A	0.04	15
ZPPR 145	Batch 2	190.1	219	Burning Curve	15°C/min	N/A	162	Linear	1.00E-01	N/A	4.9	15
ZPPR 146	Batch 2	179.1	205	Isothermal	35	500	N/A	Erratic[a]	N/A	N/A	0.31	15
ZPPR 147	Batch 2	179.1	205	Isothermal	125	300	N/A	Decreasing Rate	N/A	7.30E-07	2.86	15
ZPPR 148	Batch 2	179.1	205	Burning Curve	15°C/min	N/A	191	Linear	5.00E-02	N/A	4.6	15
ZPPR 149	Batch 2	171.9	192	Isothermal	35	500	N/A	Erratic[a]	N/A	N/A	0.31	15
ZPPR 150	Batch 2	171.9	192	Isothermal	140	100	N/A	Decreasing Rate	N/A	1.70E-06	3.02	15
ZPPR 151	Batch 2	171.9	192	Burning Curve	15°C/min	N/A	205	Linear	3.10E-02	N/A	4.3	15
ZPPR 152	Batch 2	151.3	165	Isothermal	35	300	N/A	Decreasing Rate	N/A	5.90E-08	0.38	15
ZPPR 153	Batch 2	151.3	165	Isothermal	75	600	N/A	Linear	N/A	3.20E-08	0.2	15
ZPPR 154	Batch 2	151.3	165	Burning Curve	15°C/min	N/A	176	Linear	8.60E-02	N/A	3.7	15
ZPPR 155	Batch 2	187.0	205	Isothermal	35	500	N/A	Linear	N/A	4.40E-08	0.34	15
ZPPR 156	Batch 2	187.0	205	Isothermal	100	300	N/A	Linear	N/A	2.40E-07	0.85	15
ZPPR 157	Batch 2	187.0	205	Burning Curve	15°C/min	N/A	172	Linear	8.20E-02	N/A	4.6	15
ZPPR 158	Batch 2	179.7	210	Isothermal	35	300	N/A	Linear	N/A	5.70E-08	0.2	16
ZPPR 159	Batch 2	179.7	210	Isothermal	50	3600	N/A	Erratic[b]	N/A	6.20E-09	0.1	16
ZPPR 160	Batch 2	179.7	210	Burning Curve	15°C/min	N/A	165	Linear	1.10E-01	N/A	4.7	16

a: Erratic rate too low for meaningful measurement.

b: Meaningful rate obtained by extended test duration.

Notes: Hydride fraction shown is the total initial hydride fraction in the sample, computed from the sum of weight gains in the isothermal and burning curve tests. All burning curve tests performed in Air-5%Ar at 200 ml/min.

TABLE A-VI. Test matrix and results for varying sample size tests in Ar-20%O_2

Test ID	Material	Sample Weight (mg)	Hydride Surface (cm^2)	Test Type	Ramp Rate (°C/min)	Ignition Temp. (°C)	Kinetics	Burning Rate (mg/sec)	Wt. Gain (mg)	Hydride Fraction (%)
FMFVLT 13	RAM97-23/24	129.3	270	Burning Curve	15	156	Linear	1.00E-01	5.4	25
FMFVLT 14	RAM97-23/24	148.3	290	Burning Curve	15	153	Linear	8.30E-02	5.8	23
FMFVLT 15	RAM97-23/24	130.6	245	Burning Curve	15	157	Linear	7.40E-02	4.9	22
FMFVLT 50	RAM97-23/24	240.6	460	Burning Curve	15	152	Linear	1.00E-01	9.2	23
FMFVLT 51	RAM97-23/24	275.0	425	Burning Curve	15	157	Linear	9.90E-02	8.5	18
FMFVLT 52	RAM97-23/24	207.1	330	Burning Curve	15	158	Linear	9.20E-02	6.6	19
FMFVLT 53	RAM97-23/24	99.0	140	Burning Curve	15	179	Linear	8.20E-02	2.8	17
FMFVLT 54	RAM97-23/24	94.3	130	Burning Curve	15	186	Linear	6.80E-02	2.6	16
FMFVLT 55	RAM97-23/24	68.7	100	Burning Curve	15	191	Linear	5.70E-02	2.0	17
FMFVLT 56	RAM97-23/24	79.0	115	Burning Curve	15	187	Linear	5.70E-02	2.3	17
FMFVLT 57	RAM97-23/24	52.4	75	Burning Curve	15	194	Linear	4.90E-02	1.5	17
FMFVLT 58	RAM97-23/24	51.8	75	Burning Curve	15	202	Linear	5.60E-02	1.5	17
FMFVLT 59	RAM97-23/24	27.2	40	Burning Curve	15	219	Linear	3.50E-02	0.8	18
FMFVLT 60	RAM97-23/24	25.7	38	Burning Curve	15	N/A*	N/A	N/A	N/A	N/A
FMFVLT 61	RAM97-23/24	297.5	485	Burning Curve	15	155	Linear	1.00E-01	9.7	19

*: Sample did not ignite.

Distribution for ANL-99/21

Internal:

R.J. Briggs
D.H. Cho
D.C. Crawford
S.L. Hayes
B.A. Hilton
J.R. Krsul
R.G. Pahl
D.L. Porter
C.W. Solbrig
T.C. Totemeier (10)
D. Wachs
L.C. Walters
TIS Files

External:
R. Bratton (BBWI)
M.A. Ebner (BBWI)
R.E. Felt (DOE-EH)
DOE-OSTI (2)
ANL-E Library
ANL-W Library